Stability of Zircon U-Pb Systematics in a Greenschist-Grade Mylonite: An Example from the Rockfish Valley Fault Zone, Central Virginia, USA
Author(s): David M. Wayne and A. Krishna Sinha
Source: *The Journal of Geology*, Vol. 100, No. 5 (Sep., 1992), pp. 593-603
Published by: The University of Chicago Press
Stable URL: http://www.jstor.org/stable/30068531
Accessed: 26/06/2014 13:00

# Stability of Zircon U-Pb Systematics in a Greenschist-Grade Mylonite: An Example from the Rockfish Valley Fault Zone, Central Virginia, USA[1]

*David M. Wayne*[2] *and A.Krishna Sinha*

*Department of Geological Sciences, Virginia Tech, Blacksburg, VA, 24061, USA*

**ABSTRACT**

The mid-Paleozoic, greenschist-grade Rockfish Valley Fault Zone (RVFZ) of central Virginia cuts the Grenville-aged Pedlar River Charnockite Suite (PRCS) and contains zircons that underwent brittle failure during ductile deformation. Electron microprobe analyses and scanning electron microscope (SEM) backscattered electron (BSE) imaging show that zircons from the protolith PRCS are concentrically zoned (with alternating U-Hf-rich and U-Hf-poor bands), and contain numerous radial microcracks. Zircons from the RVFZ mylonite are unzoned, fragmented, show no internal microfractures, and have low U and Hf concentrations relative to the PRCS zircons. U-Pb isotopic studies of zircons from the mylonites and from the charnockitic protolith demonstrate that no preferential Pb loss occurred in the zircons from the mylonite, and that the $^{207}Pb/^{206}Pb$ ages of the mylonite zircons are identical to those of the protolith zircons. The loss of primary zoning from the zircons of the RVFZ ultramylonites can be explained by the physical removal of microfractured, U-rich, alpha-damaged zircon domains as the result of brittle failure and disaggregation during mylonitization. Mechanically resistant (low-U) portions of zircon grains tended to remain intact in the mylonite. Thus, it may not always be possible to predict whether or not the zircon U-Pb system has been disturbed by mylonitization by using physical criteria (e.g., grain size reduction, obliteration of primary zoning textures) alone. Evidently, fluids present during mylonitization accomplished the hydration of primary mineral assemblages, but did not chemically interact with zircons, and their primary U-Pb and Pb-Pb ages were preserved.

## Introduction

Studies of zircon U-Pb isotopic systematics in mylonites (Lindh and Schoberg 1988; Scharer 1978; Sinha and Glover 1978; Wayne and Sinha 1988; Wayne et al. 1992) suggest that the ability of zircon to date metamorphism is dependent on both its mechanical behavior during grain size reduction and its chemical response to fluid-rock interaction and metamorphic reactions. In many instances, zircons from mylonites are appreciably more discordant than those from the less-deformed protolith (e.g., Lindh and Schoberg 1988). Isotopic discordance occurs when Pb, U, and/or Th is lost (or gained) at some time after primary crystallization. In zircon, Pb loss is prevalent over other discordance-producing mechanisms because alpha-decay events (which produce radiogenic Pb) cause extensive internal structural disorder (e.g., Chakoumakos et al. 1987; Murakami et al. 1991). Zircon damaged by alpha-decay events is thus less able to retain the daughter product during episodes of heating and/or fluid-rock interaction.

Brittle failure of zircon during mylonitization has been documented (Boullier 1980; Wayne and Sinha 1988; Lindh and Schoberg 1988; Dirks and Hand 1990). Although fracturing, by itself, does not necessitate Pb-loss (e.g., Aaberg and Bollmark 1985), it may facilitate Pb loss in several ways: (1) by increasing the surface area available for leaching by metamorphic fluids, (2) by providing additional high-diffusivity paths that may enhance the mobility of radiogenic Pb, and (3) by decreasing the effective radius for diffusion of Pb out of the zircon.

The presence of pre-existing microcracks may influence the deformation behavior of a material (e.g., during mylonitization) by providing sites for the nucleation of dynamically induced cracks (Atkinson 1982). Thus, the occurrence of microcracks in zircon (a common feature of radiation-damaged materials; see Clinard and Hobbs 1986) prior to the

[1] Manuscript received November 12, 1991; accepted March 30, 1992.

[2] Present address: Department of Earth Sciences, the University, Leeds, England LS2-9JT.

[The Journal of Geology, 1992, volume 100, p. 593–603]  0022-1376/92/10005-0010$1.00

onset of mylonitization may enhance its tendency toward brittle behavior. Studies of synthetic and natural materials suggest that microcracking in zircon is related to anisotropic lattice expansion caused by the accumulation of interstitial atoms displaced primarily by alpha-recoil events (Clinard and Hobbs 1986; Chakoumakos and Ewing 1985; Murakami et al. 1991). The formation of microcracks in natural, radiation-damaged zircons may be facilitated by chemical zonation of U and Th (Chakoumakos et al. 1987, 1992), where the accumulation of lattice defects proceeds at different rates in the radionuclide-poor and radionuclide-rich portions of the crystal. Interstitial defects accumulate more rapidly in the radionuclide-rich zones, causing lattice expansion to proceed at a faster rate, relative to the rate of expansion in the radionuclide-poor zones. This differential swelling, in turn, sets up an internal stress field that may cause microfracturing (Chakoumakos et al. 1987). Thus, chemically zoned, microfractured zircons may be predisposed to extensive grain-size reduction via further fracturing and physical disaggregation during mylonitization.

The objective of the present study was to examine the possible relationships between the U-Pb isotopic systematics of zircon and its mechanical behavior at greenschist-grade conditions. To this end, we performed a detailed chemical and isotopic study of zircons in mylonites from the Rockfish Valley Fault Zone (RVFZ) in central Virginia. The RVFZ mylonites are derived from the Grenville-aged Pedlar Charnockite (Sinha and Bartholomew 1984), which contains abundant, large, chemically zoned zircons.

## Geologic Setting

Located in the Blue Ridge of central Virginia (figure 1), the Pedlar River Charnockite Suite (PRCS) is a complex association of Grenville-aged granulite-grade metasediments and igneous rocks. The charnockite is coarse-grained, granoblastic, and consists of quartz, alkali feldspar, plagioclase, biotite, and orthopyroxene. Accessory phases (magnetite/ilmenite, zircon, and apatite) are abundant, and locally the rock shows signs of low-temperature alteration, particularly along fractures. Euhedral, concentrically zoned zircons typically occur in association with apatite and clusters of subhedral opaques which are, themselves, intimately associated with orthopyroxene and biotite. Less often, zircon occurs as inclusions within quartz and feldspars. The results of previous geochronologic studies of the PRCS and related rocks are summarized in table 1 (see also: Davis 1974; Pettingill et al. 1984; Sinha and Bartholomew 1984; Bartholomew et al. 1991).

The Rockfish Valley Fault Zone (RVFZ) (figure 1) constitutes the southeastern border of the parautochthonous PRCS (Bartholomew et al. 1981). At the sample locality, the RVFZ is composed of a series of small ductile deformation zones (Mitra 1978; Bartholomew et al. 1981), which vary in width from <1 cm to approximately 100 m. Samples for U-Pb geochronology were obtained from the widest portion of this zone. Deformation within the ductile deformation zones (DDZs) is inhomogenous, and mildly deformed felsic gneisses are crisscrossed by narrow zones (>1 to 4 cm) of fine-grained mylonitic material. Across these zones, the reduction in grain size is accompanied by an increase in the modal proportions of phyllosilicates (chlorite, green biotite and white mica), calcite, epidote-group minerals, and actinolite at the expense of feldspars, orthopyroxene, and red-brown biotite. The hydrated, phyllosilicate-rich mineral assemblages pervasively developed throughout the ultramylonites of the RVFZ indicate that deformation and metamorphism of the charnockite took place at greenschist-grade conditions in the presence of a $H_2O$-rich fluid phase (see also Mitra 1978; Bartholomew et al. 1981). Zircon is abundant in the mylonites as rounded or broken grains.

Deformation within the RVFZ is inferred to be middle Paleozoic (450–475 Ma) in age, primarily on the basis of field relationships (Bartholomew et al. 1981, 1991; Pettingill et al. 1984). Dallmeyer (1975) also obtained mid-Paleozoic ages for a retrograde event in the southern Blue Ridge basement using $^{39}Ar/^{40}Ar$ data from biotite and hornblende. A Rb-Sr whole rock study (Pettingill et al. 1984) of the mylonitized charnockite from the RVFZ (also used to obtain zircon for this study) indicated that mylonitization caused only partial redistribution of Rb and Sr.

## Analytical Techniques

Chemical analyses of zircons were performed at Virginia Tech and the University of Leeds on automated Cameca SX-50 4-channel electron microprobes. Counting statistics yield detection limits in the range of 0.005 to 0.01 wt % oxide for each of the trace elements, with the exception of Yb and Er, which have detection limits of 0.01 to 0.015 wt % oxide. Details on the operating conditions, analytical standards, counting times, and other microprobe procedures used are presented in Wayne

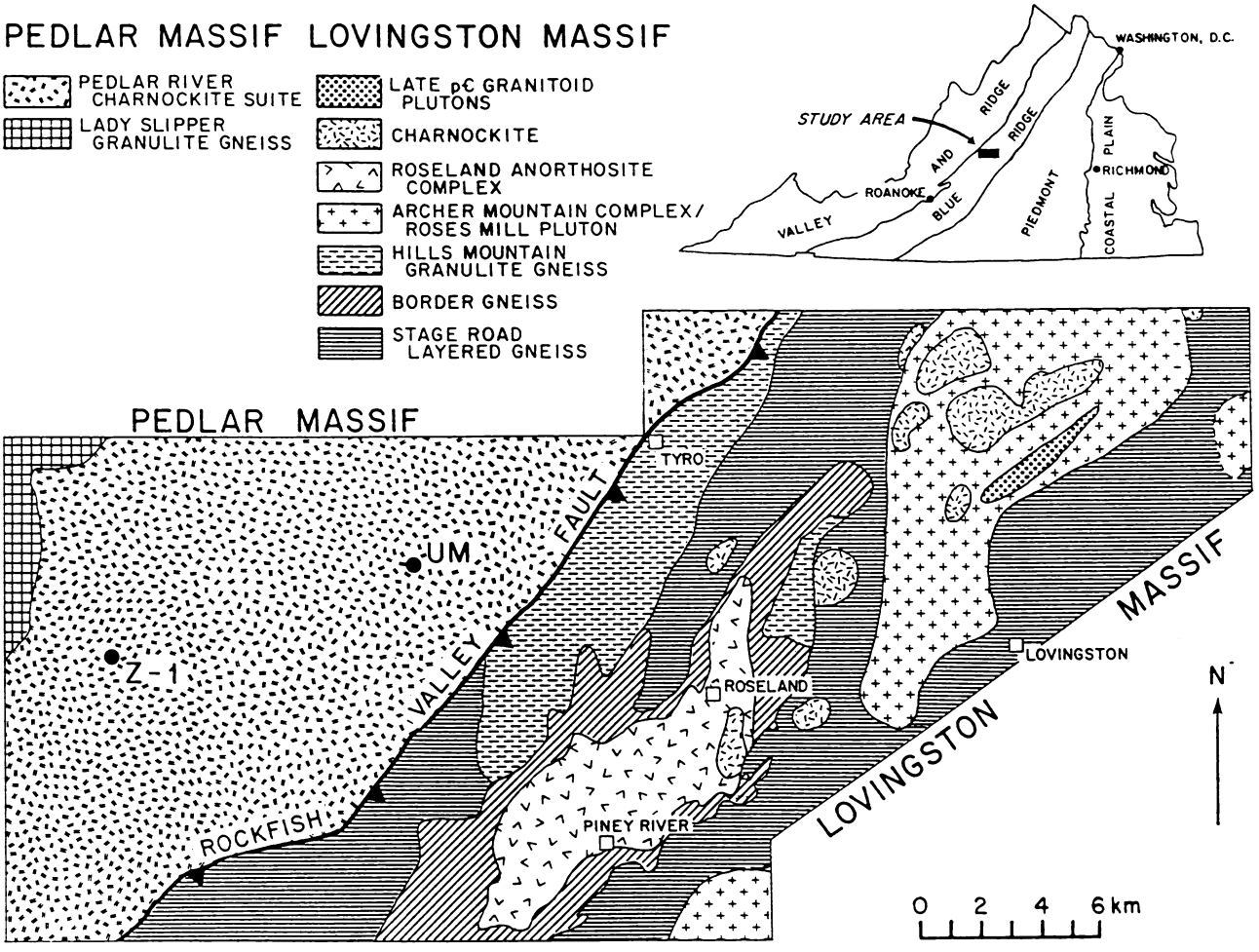


**Figure 1.** Geologic map of the central Virginia Blue Ridge (adapted from Pettingill et al. 1984), showing the location of the charnockite sample (Z-1) and the mylonitized charnockite (UM) from the RVFZ.

(1990) and Wayne et al. (1992). SEM work included both secondary electron imaging (SEI) for information on surface features and backscattered electron (BSE) images for information on variations in mean atomic number (Z-number) within single zircon grains. Details on the application of these techniques are presented in Lloyd (1987) and Paterson et al. (1989). For mass spectrometry, zircon fractions were separated from fresh 45–90 kg rock samples via standard mineral separation techniques. The remaining steps in the dissolution, processing, and purification of Pb and U from zircon follow the method of Krogh (1973). All isotope ratios corrected for mass fractionation (Pb: 0.04 to 0.12% per amu, U: 0.03% to 0.08% per amu) and total procedural blank (Pb: 0.2 to 0.6 ng, U: 0.015 ng). All U/Pb and Pb/Pb age data corrected for 1030 Ma old common Pb using the two-stage evolution model of Stacey and Kramers (1975). Decay constants are from Steiger and Jaeger (1977). A more detailed account of the methods of analysis is given by Wayne (1990), and Wayne et al. (1992). Regressions were performed using ISOPLOT (Ludwig 1990*a*), with U/Pb isotopic ratios, rho values, and associated errors obtained from PBDAT (Ludwig 1990*b*). Uncertainties on upper and lower intercept ages are stated at the 95% confidence level.

## Zircon Morphology and Fracturing

Zircons from the less-deformed charnockite within the PRCS (figure 2*a*, table 2) are prismatic, subhedral, and rounded, with complex terminations; typical of zircons from charnockites (e.g., Duchesne et al. 1987). These zircons show strong variations in color: from dark brown and nearly opaque, to pale lilac and transparent. Concentric internal zoning and radial fractures are readily apparent in grains immersed in oil, and in thin section. No corrosion, surface pitting, or core-overgrowth

**Table 1.** Age Data from the Pedlar River Charnockite and Related Rocks

| Unit | Age (Ma) | Technique |
|---|---|---|
| PRCS[a] | 1021 ± 36 | Rb-Sr whole rock |
| " | 1489 ± 118 | Nd-Sm whole rock |
| " | 1189 ± 300 | Nd-Sm K-spar/whole rock join |
| RVFZ mylonite[a] | 683 ± 34 | Rb-Sr whole rock |
| PRCS[b] | 1029 | Zircon Pb/Pb age (avg.) |
| " | 1075 | Zircon U-Pb upper intercept age |

[a] Pettingill et al. (1984).
[b] Sinha and Bartholomew (1984).

**Table 2.** Zircon Morphology

| Sample | n | Avg. length (mm) | Avg. l:w ratio |
|---|---|---|---|
| PRCS charnockite | 22 | .266 ± 63 | 2.11 ± 43 |
| RVFZ mylonite, unfractured | 20 | .218 ± 35 | 2.21 ± 58 |
| RVFZ mylonite, fractured | 30 | .179 ± 25 | 1.48 ± 26 |

Note. Measurements made at 100X in transmitted light. All samples are from a single seived fraction (−100, +200). Standard deviations are 1-sigma.

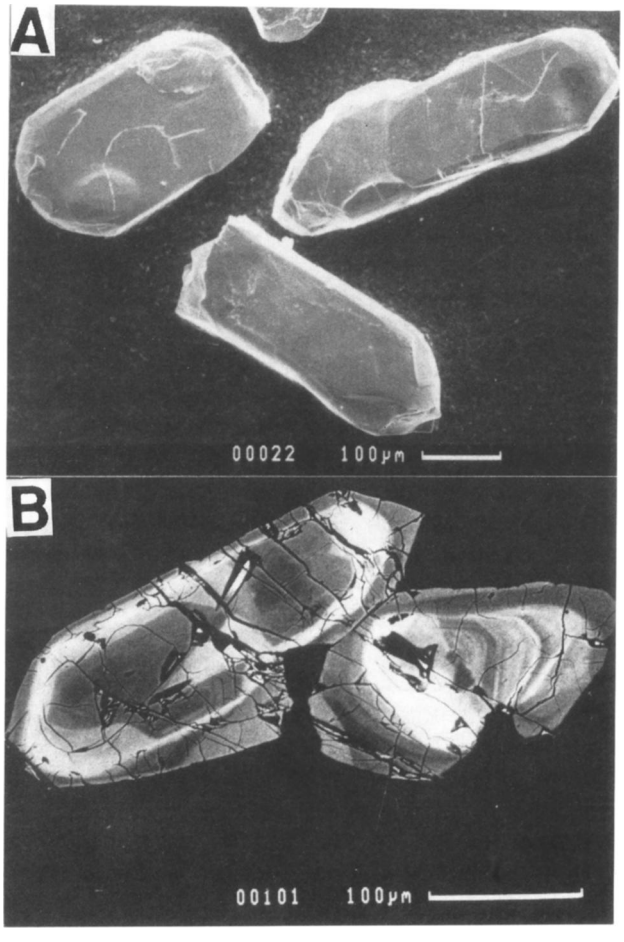


**Figure 2.** Zircons from the charnockite unit of the PRCS. (*a*) Secondary electron image (−100+200 fraction) showing complex crystal form and rounded terminations typical of zircons from charnockites. (*b*) Backscattered electron (BSE) image of zircons from a thin section of the charnockite, showing euhedral form, complex zonation, abundant internal microfractures (both radial and concentric) and crosscutting fractures (see text).

structure is evident from secondary electron images (figure 2*a*).

Zircons from the PRCS contain abundant internal fractures. We believe that these are not simply the result of sample preparation for several reasons: (1) other minerals in the PRCS samples contain few internal fractures, (2) fracturing due to thin sectioning and polishing has a distinctive appearance, and occurs only in the outermost 2–5 mm of the sample (which was avoided), (3) the radial fracture patterns of the PRCS zircons, in particular, are typical of radiation-damaged materials (see below), and (4) the fracture patterns are controlled by the zoning pattern of the zircon.

In thin section and in BSE images (figure 2*b*), at least three distinct fracture sets are apparent in zircons from the PRCS: (1) crosscutting planar cracks, (2) radial microfractures, and (3) curved internal microfractures. Typically, the crosscutting cracks penetrate through zircons and pass into adjacent mineral grains and may be filled with secondary minerals such as calcite. These cracks originated during late-stage fracturing of the charnockite, which may be related to either the late Paleozoic mylonitization, the more recent (200–300 Ma) thrusting of the Blue Ridge Province over the Valley and Ridge Province (Sinha and Bartholomew 1984), or uplift.

Radial fractures are due to internal stresses exerted by differential swelling as the result of the accumulation of point defects related to alpha-recoil damage (e.g., Chakoumakos et al. 1987). Typically, these microfractures are oriented perpendicular to the concentric zoning pattern (see also Peterman et al. 1986). From the BSE image (figure 2*b*), it is also apparent that radial microcracks die out at zone boundaries, or within zones of relatively high average Z-number (and low birefringence). This was also observed by Chakoumakos et al. (1987) in zoned Sri Lankan zircon and may be the result of crack-tip blunting brought on

by the inability of the crack to propagate through the dense tangle of dislocations and point defects present in the radiation-damaged material (Clinard and Hobbs 1986). Chakoumakos et al. (1987) also point out that such behavior is consistent with the observed decrease in the elastic moduli (Ozkan 1976; Chakoumakos et al. 1992) and increase in fracture toughness of radiation-damaged zircon.

Although their origin can only be speculated upon, the morphology of the curved internal microcracks suggests that they may also be caused by stresses related to gradients in the intensity of alpha-damage. Note that the trajectories of the curved microcracks run approximately parallel to the concentric zoning patterns visible in the BSE image (figure 2*b*) and appear to be localized near zone boundaries. Similar fracture patterns have also been observed in zoned zircons from the Brevard Fault Zone (Wayne and Sinha 1988).

Zircons from the retrograde ultramylonites of the RVFZ are pale lilac in color (some are stained yellow-brown by Fe oxides), and approximately 70% have one (or more) fracture surfaces (figure 3*a*). Unbroken crystals display the same complex terminations and rounded appearance as the zircons from the protolith and have a similar average length-width ratio to the zircons from the undeformed charnockite (table 2). For a given size fraction (e.g., −100, +200 mesh), fractured zircons from the mylonite are smaller and have lower average length-width ratios (table 2) than unfractured zircons. Secondary electron images of these zircons revealed no surface features associated with corrosion or pitting (figure 3*a*).

In thin section, zircons from the RVFZ are commonly rounded (figure 3*b*) and/or fragmented (figure 3*c,d,e*). Some grains shown boudinage-type structures (figure 3*b*), which are consistent with brittle failure in a dominantly tensional stress regime (Lloyd and Ferguson 1981). Boudinaged zircons are typically fractured along planes oriented at high angles to the foliation, with the widest fracture-spacing at the center of the grain (figure 3*b*). Inter-boudin gaps are filled with matrix material. These extensional fracture patterns are similar to those produced by brittle failure via stress transfer (White et al. 1980), whereby tensional stresses are exerted on a brittle mineral grain (in this case: zircon) by the ductilely deforming matrix. The maximum stress is localized at the center of the mineral grain, and fractures form perpendicular to the axis of maximum tensile stress. Thus, elongated grains tend to break at the center into roughly equidimensional segments. The operation of a stress transfer mechanism is also consistent with the observed reduction in length : width ratio of the fractured zircons from the RVFZ (see also Boullier 1980).

## Zircon Chemistry

Zircons from the PRCS are typified by complex, concentric zoning (e.g., figure 2*b*), and the average Z-number contrast apparent in BSE images corresponds to birefringence contrasts visible in thin section. Zones with relatively low birefringence (1° yellow to red) correspond to zones of brightness in the BSE, and highly birefringent zones (2° green) correspond to dark zones in the BSE. This suggests that the contrasts in average Z are related to changes in the total alpha-decay dose of the different zones by virtue of their relatively high contents of high Z-number substituents (e.g., U, Th), an observation also confirmed by microprobe analyses (see also Sahama 1981; Chakoumakos et al. 1987).

A table (Table 3) containing the complete microprobe analyses of the RVFZ and PRCS zircons can be obtained from *The Journal of Geology* upon request, free of charge. Microprobe analyses of zircon from the PRCS demonstrate a strong correlation between BSE intensity and the relative concentration levels of trace elements (figure 4). The "bright" zones consistently contain greater amounts of $UO_2$, $HfO_2$, and $Yb_2O_3$ than do the dull zones. The elevated U content of the bright zones is also consistent with their lower birefringence, caused by the accumulation of lattice defects due to alpha-decay (e.g., Holland and Gottfried 1955; Sahama 1981; Chakoumakos et al. 1987).

By contrast, BSE images of the zircons from the RVFZ (figure 3*b,c,d*) reveal a lack of sharp compositional gradients. Patterns of Z-number contrast are diffuse and poorly defined, although zircons from the RVFZ may bear remnants of zones having sharp, well-defined Z-number contrasts on their outer perimeters (e.g., figure 3*b*). Microprobe analyses also indicate that zircons from the RVFZ generally lack regions of high U content (figure 4). The chemistry of zircons from the mylonite tends to be similar in terms of $HfO_2$ and $UO_2$ content to the "dull" regions of zircons from the PRCS (table 3, figure 4). Analyses of the zircon fragments shown in figure 3 (*d*) and (*e*) group with the low-U, low-Hf population (figure 4).

## Isotopic Analyses

The U-Pb isotopic data for zircons from the PRCS were originally presented in Sinha and Bartholomew (1984). For this study, their raw isotopic data

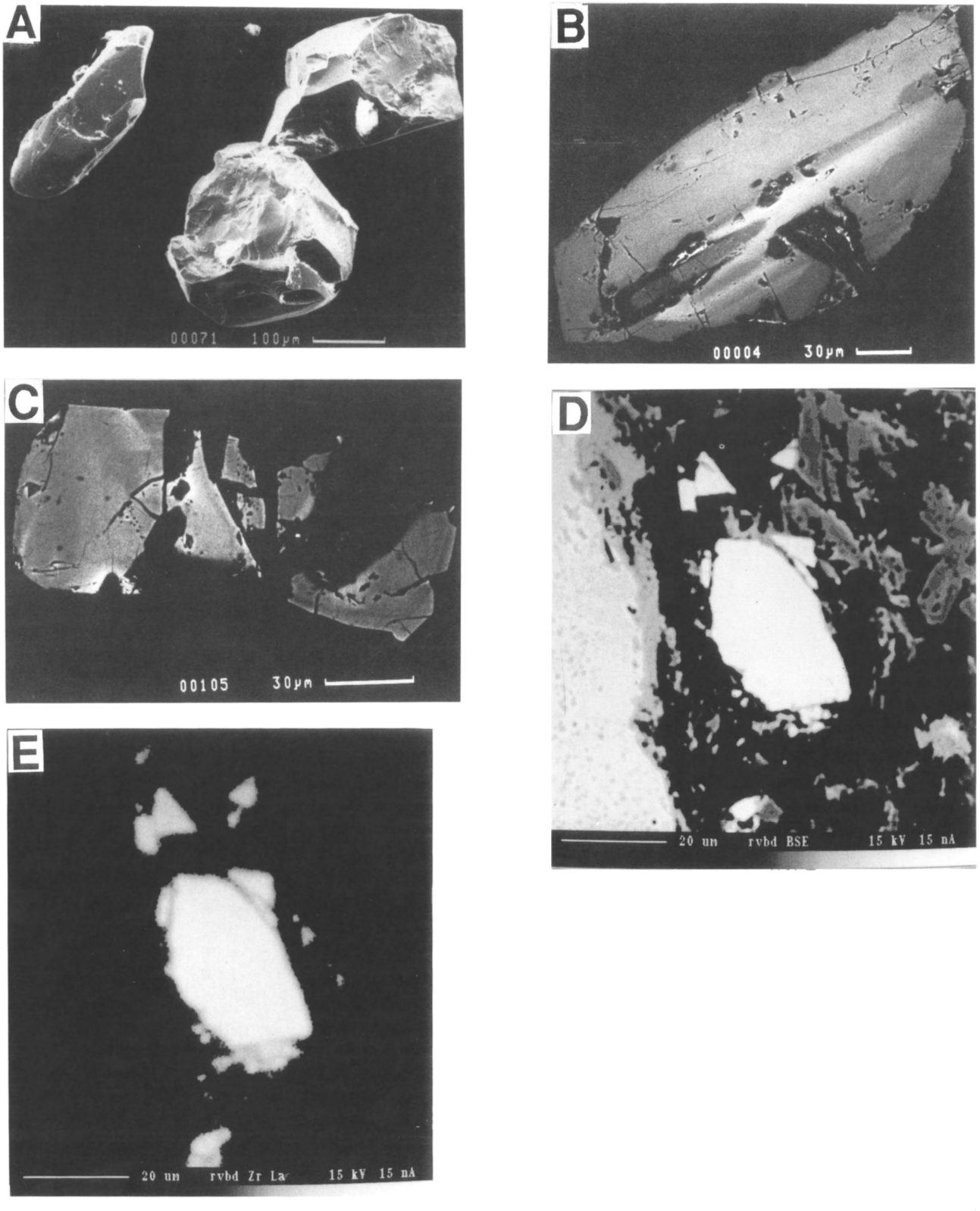


**Figure 3.** Zircons from the greenschist-grade mylonites of the Rockfish Valley Fault Zone (RVFZ). (*a*) Secondary electron image of zircons (−100 + 200 fraction). Zircons with one or more fracture surfaces are abundant, but evidence of surface pitting and corrosion is lacking. (*b*), (*c*) and (*d*) BSE images of zircon from a thin section of the RVFZ mylonite. Mylonitic foliation is parallel to the long axis of the photograph in (*c*), and parallel to the long axis of the zircon in (*b*) and (*d*). Note the absence of pronounced, regular zoning patterns in all three images. (*c*) and (*d*) show the development of boudinage-type structures, and the fragmentation of zircon grains. (*e*) Zr Lα emission map of the area depicted in (*d*).

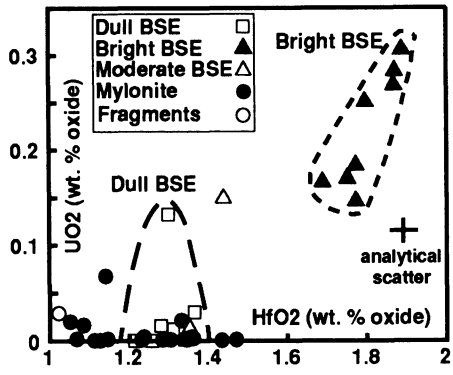


**Figure 4.** Variation of $UO_2$ vs. $HfO_2$ in zircons from the protolith charnockite of the PRCS (solid squares, hollow squares, hollow triangles) and the RVFZ mylonite (solid and hollow circles). In the PRCS zircons, analyses of zones with high average Z-number ("bright" zones) cluster tightly in the high $UO_2$-high $HfO_2$ region, while analyses of zones having lower average Z-number ("dull" zones) tend to have lower U and Hf contents. Hf and U contents of zircons and zircon fragments from the RVFZ are similar to those of the "dull" zones of the PRCS.

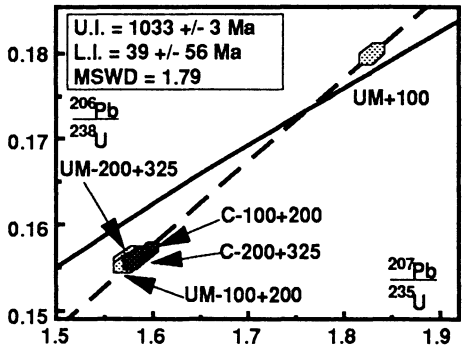


**Figure 5.** Concordia plot of zircon U-Pb data from the PRCS (Sinha and Bartholomew 1984), and the RVFZ. Note that none of the data from the RVFZ is rotated toward the age of mylonitization (approx. 450 Ma). Error polygons represent 2-sigma uncertainties, while the errors on the upper and lower intercept ages are stated at the 95% confidence interval.

was reprocessed using PBDAT (Ludwig 1990*b*) and presented in table 4. New U-Pb isotopic data were collected on three mesh size fractions (+100, −100+200, −200+325) obtained from the charnockite-derived retrograde mylonites of the RVFZ. Fractions finer than 325 mesh were not recoverable due to the extremely fine grain size (< 25 μm) of the enclosing mylonite.

The close correspondence of the $^{207}Pb/^{206}Pb$ ages of the zircons from the charnockite and the retrograde ultramylonite (table 4, and figure 5) indicates that the zircon U-Pb system remained closed during the greenschist-grade event. The isotopic data from the three size fractions obtained from the mylonite, combined with the data from the charnockite, yield a well-constrained upper intercept age of 1033 ± 3 Ma and a lower intercept of 40 ± 52 Ma (figure 5). The upper intercept age is in close agreement with the whole rock Rb-Sr age of 1021 Ma, obtained by Pettingill et al. (1984) and the results ($^{207}Pb/^{206}Pb$ ages: 1027–1031 Ma) of the study by Sinha and Bartholomew (1984). Note, however, that the data points representing the charnockite zircons and two of the three mylonite fractions are tightly clustered (figure 5). When combined with the data from the +100 RVFZ ultramylonite zircons, the result is a line based on two points. The slight reverse discordance of the +100 RVFZ zircons is probably the result of minor present day

**Table 4.** U-Pb Isotopic Data

| Sample | U (ppm) | Pb (ppm) | Atomic Ratios $^{206}Pb^b/^{204}Pb$ | $^{207}Pb^b/^{206}Pb$ | $^{206}Pb^b/^{208}Pb$ | $^{207}Pb^c/^{235}U$ | $^{206}Pb^c/^{238}U$ | $^{207}Pb^c/^{206}Pb$ | Ages (Ma) $^{206}Pb/^{238}U$ | $^{207}Pb/^{235}U$ | $^{207}Pb/^{206}Pb$ |
|---|---|---|---|---|---|---|---|---|---|---|---|
| *Charnockite*[a] | | | | | | | | | | | |
| PC−100+200 | 273 | 43 | 9,237 | .07526 | 10.0200 | 1.5948 | .15690 | .07372 | 940 | 968 | 1034 ± 4 |
| PC−200+325 | 286 | 45 | 10,108 | .07499 | 9.8943 | 1.5826 | .15601 | .07358 | 935 | 963 | 1030 ± 2 |
| *Ultramylonite* | | | | | | | | | | | |
| RV+100 | 190 | 36 | 9,666 | .07521 | 7.0756 | 1.8281 | .17980 | .07374 | 1066 | 1056 | 1034 ± 2 |
| RV−100+200 | 185 | 31 | 2,979 | .07820 | 6.2130 | 1.5735 | .15544 | .07342 | 931 | 960 | 1026 ± 12 |
| RV−200+325 | 181 | 30 | 2,736 | .07848 | 6.0409 | 1.5774 | .15614 | .07327 | 935 | 961 | 1022 ± 14 |

Note. All samples represent the least magnetic fraction at 1.75 amperes, 9 degrees forward tilt and 2 degrees side tilt on the Frantz isodynamic separator.
[a] See also Sinha and Bartholomew (1984).
[b] Corrected for blank and mass fractionation.
[c] Corrected for blank, mass fractionation and common Pb.

U-loss induced by a prolonged (45 min.) washing step in warm 8N TD-$HNO_3$ undertaken to remove surface contamination and Fe oxide staining. Despite the potential U-loss during the acid wash, the $^{207}Pb/^{206}Pb$ ratio of the +100 RVFZ fraction is similar to that of the remaining samples.

To test the validity of the intercept ages, the data set was regressed (1) without the RVFZ +100 point, (2) without RVFZ +100, but with the upper intercept forced at 1021 Ma (the Rb-Sr whole rock agr obtained by Pettingill et al. 1984), and (3) without RVFZ +100, but with the lower intercept forced at 0 ± 10 Ma. The results of all regressions are shown in table 5. The unconstrained data yield statistically and geologically meaningless "ages" due to the lack of spread in U/Pb ratios. By contrast, the relatively good fit of the zircon data to the forced upper intercept of 1021 Ma (and the resulting 0 Ma lower intercept age) are consistent with the results of the regression which included the +100 RVFZ data. Similarly, the forced fit through a 0 Ma lower intercept yields a geologically reasonable upper intercept age of 1030 ± 8 Ma. Thus, the inclusion of the RVFZ +100 data creates no bias in upper or lower intercept ages.

Bulk uranium concentration data obtained via isotope dilution are consistent with the results of the electron microprobe analyses summarized in the preceding section. The two size fractions of zircons from the charnockite protolith contain 273 and 286 ppm U, while the three zircon fractions from the RVFZ ultramylonite contain 181 to 190 ppm U. Similarly, the Pb concentrations of the charnockite zircons (43 to 45 ppm) are also slightly higher than those of the ultramylonite zircons (30 to 36 ppm). These compositional trends may be related to: (1) primary heterogeneities in the U (and Pb) content of different zircon populations, or (2) grain size reduction of zircons during mylonitization, resulting in the preferential degredation of U-Th-rich, microfractured zircons.

**Table 5.** Regression Results of Zircon U-Pb Data

| Regression parameters | U.I. (Ma) | L.I. (Ma) | MSWD |
|---|---|---|---|
| 5 points (all data) | 1033.4 ± 3.2 | 39 ± 56 | 1.79 |
| 4 points, no constraints | 1407 ± 874 | 804 ± 402 | .52 |
| 4 points, U.I. at 1021 10 Ma | . . . | 146 ± 230 | 3.3 |
| 4 points, L.I. at 0 ± 10 Ma | 1030 ± 7.5 | . . . | 2.8 |

## Discussion

The zircon U-Pb isotopic data from PRCS charnockite and the RVFZ ultramylonites suggest that the geochemical and physical processes associated with mylonitization at greenschist grade do not necessitate the preferential loss of radiogenic Pb. At first glance, this seems to be at odds with the results of BSE imaging, which revealed the absence of primary concentric zoning features in the RVFZ zircons. Such zoning patterns may be partially obliterated by annealing of alpha-recoil damage, or diffusion of U, Th, Hf, and other substituents during a thermal episode. Recrystallization and annealing of metamict zircon during greenschist-grade metamorphism is known to occur (Gebauer and Grunenfelder 1976) but would require partial (if not total) resetting of the U-Pb isotopic system during the event. Similarly, the energy required for substantial diffusive transport of large, highly charged cations such as U, Hf, and Th would far exceed that required to activate radiogenic Pb atoms, which reside in loosely bound, disordered sites due to alpha-recoil damage.

Hydrothermal experiments (e.g., Pidgeon et al. 1966; Sinha et al. 1989; Hansen and Friderichsen 1989) have also shown that interaction of zircons with saline fluids and dilute acids at elevated P-T conditions results in severe Pb loss and, in some cases, partial dissolution. Zircons from the RVFZ totally lack surface features indicative of dissolution (e.g., Wayne et al. 1992). This suggests that the critical factor in the preservation of zircon $^{207}Pb/^{206}Pb$ ages in the RVFZ was the inability of the fluids present during mylonitization to leach radiogenic Pb from severely alpha-damaged regions of zircon grains. Such "passive" behavior of the zircon U-Pb system has also been observed in other retrograde mylonites, such as the Bitterroot mylonite zone (Chase et al. 1983). This generalization cannot be extended to include all retrograde mylonites, as perturbation of the zircon U-Pb system due to greenschist-grade mylonitization has been documented by Scharer (1978), Gehrels and Saleeby (1987), Lancelot et al. (1983), and Lindh and Schoberg (1988). In two of these examples (Lancelot et al. 1983; Lindh and Schoberg 1988), however, surface corrosion and pitting of zircons from the mylonites was observed using SEM techniques.

Although the instance of primary heterogeneity cannot be ruled out, the results of the microprobe study and the isotopic dilution analyses, together with the textural evidence for brittle deformation of the zircons in the RVFZ ultramylonite, suggest

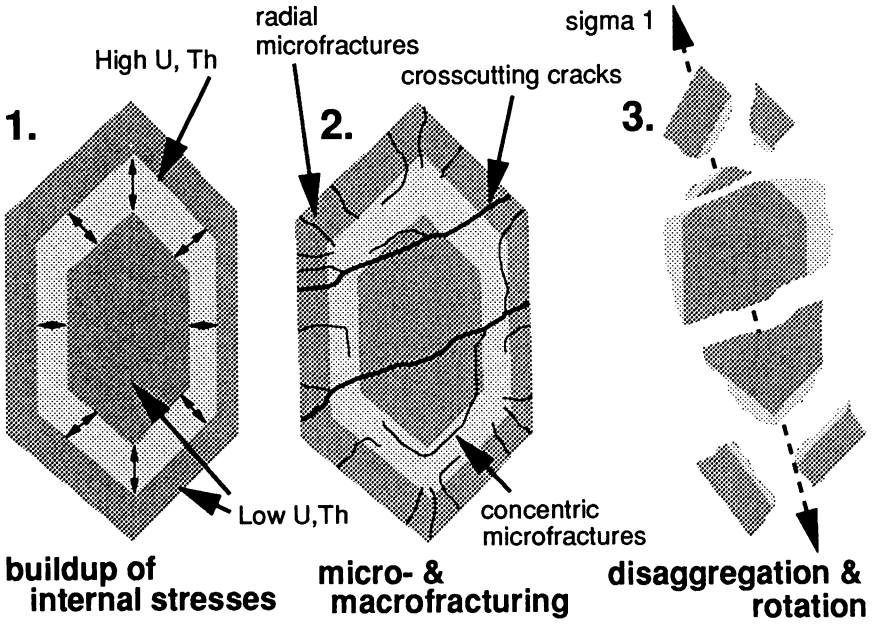


**Figure 6.** Steps in the physical evolution of zircon in the RVFZ. *Step 1:* Internal stresses build as zircon undergoes anisotropic lattice expansion due to alpha-recoil damage. U-Th rich zones expand at a faster rate than U-Th poor zones, resulting in additional stress buildup at zone interfaces. *Step 2:* Radial microfractures develop as a result of stress buildup. Crosscutting cracks may also occur in response to external stresses. *Step 3:* Fragmentation and disaggregation of zoned, microfractured zircon during mylonitization. Note that individual fragments show little of the original zoning pattern.

that their lower U concentrations may be a result of the disaggregation of zoned zircons during mylonitization (figure 6). In this model the mechanical behavior of zircons constituting an initially heterogenous population (i.e., U-rich and U-poor) may be very different, and zoned, microfractured U-rich zircons would be preferentially disaggregated during mylonitization while pristine U-Th-poor zircons remained relatively intact. The U-rich portions of zoned zircons, already riddled with microcracks due to the effects of alpha-recoil damage, act as sites for crack nucleation and growth in an external stress field. Further stress increases may cause fragmentation and total disaggregation of the entire zircon crystal via stress transfer, depending on its size and orientation.

Fracturing and comminution of zircons during mylonitization along the RVFZ resulted in the formation of a fine grained (<20 μm) zircon population, composed exclusively of fragments (e.g., figure 3*d*,*e*). The fine grain size of the mylonite itself precluded the recovery of this fraction for U-Pb isotopic work. Microprobe analyses of two fragments revealed no unusually high U concentrations, as predicted by our model (figure 6). If these fragments are representative of the majority of zircon fragments in the ultramylonite, we suggest that the exfoliation of U-rich fragments occurred at an early stage in the deformational history of the mylonite zone. Thus, within the ultramylonites, the removal of external U-rich zones may already have been accomplished and further deformation resulted in the disaggregation of mechanically competent U-poor zircon. Therefore, future investigations of the isotopic, chemical and mechanical behavior of zircon in deformed rocks should include detailed studies of protomylonites as well as ultramylonites.

## Conclusions

1. Paleozoic mylonitization of Grenville-aged charnockite from the PRCS at greenschist-grade caused no disruption of zircon U-Pb isotopic systematics.

2. Zircons from the RVFZ show evidence for extensive brittle failure and fragmentation as a result of mylonitization. Unlike zircons from the protolith charnockite, zircons from the RVFZ are not chemically zoned. Therefore, the loss of primary zoning in fractured zircons from the RVFZ is associated with a mechanical process that did not disrupt U-Pb systematics.

3. We suggest that microfracturing related to alpha-decay damage predisposed zoned zircons to brittle failure and exfoliation of U-rich zones during mylonitization.

4. Geochronologic studies of zircons from metamorphic rocks should include a detailed SEM study of their surface features and zoning patterns. From the available data, it appears that the disturbance of zircon U-Pb systematics in mylonites is associated with surface corrosion and/or overgrowths.

## ACKNOWLEDGMENT

This research was supported by grants from NSF (EAR 8416575) and DOE (Division of Basic Energy Research, Contract DE-FGO5-88-ER13951). Hal Pendrak maintained the mass spectrometer, and Todd Solberg assisted in the microprobe lab at Virginia Tech. Eric Condliffe (Leeds) performed some of the microprobe analyses, and acquired the Zr map. Martin Dodson, Bob Cliff, and Geoff Lloyd reviewed early drafts of this paper, and their critical comments are greatly appreciated. Journal reviews by Rodney C. Ewing and an anonymous reviewer are gratefully acknowledged.

## REFERENCES CITED

Aaberg, G., and Bollmark, B., 1985, Retention of U and Pb in zircons from shocked granite in the Siljan impact structure, Sweden: Earth Planet. Sci. Lett., v. 74, p. 347–349.

Atkinson, B. K., 1982, Subcritical crack propagation in rocks: theory, experimental results and applications: Jour. Struct. Geol., v. 4, p. 41–56.

Bartholomew, M. J.; Gathright, T. M.; and Henika, W. S., 1981, A tectonic model for the Blue Ridge of Central Virginia: Am. Jour. Sci., v. 281, p. 1164–1183.

———; Lewis, S. E.; Hughes, S. S.; Badger, R. L.; and Sinha, A. K., 1991, Tectonic history of the Blue Ridge basement and its cover, central Virginia, *in* Schultz, A., and Compton-Gooding, E., eds., Geologic Evolution of the Eastern United States: Field Trip Guidebook, NE-SE GSA 1991, VMNH Guidebook 2, p. 57–90.

Boullier, A. M., 1980, A preliminary study on the behavior of brittle minerals in a ductile matrix: example of zircon and feldspars: Jour. Struct. Geol., v. 2, p. 211–217.

Chakoumakos, B. C., and Ewing, R. C., 1985, Anisotropic lattice deformation in crystals due to alpha-decay damage: Geol. Soc. America Abs. with Prog., v. ?, p. 542.

———; Murakami, T.; Lumpkin, G. R.; and Ewing, R. C., 1987, Alpha-decay-induced fracturing in zircon: the transition from the crystalline to the metamict state: Science, v. 236, p. 1556–1559.

———; Oliver, W. C.; Lumpkin, G. R.; and Ewing, R. C., 1992, Hardness and elastic modulus of zircon as a function of heavy-particle irradiation dose: I. *In situ* alpha-decay event damage: Radiation Effects and Defects in Solids, in press.

Chase, R. B.; Bickford, M. E.; and Arruda, C. E., 1983, Tectonic implications of tertiary intrusion and shearing within the Bitterroot dome, northeastern Idaho batholith: Jour. Geology, v. 91, p. 462–470.

Clinard, F. W., and Hobbs, L. W., 1986, Radiation effects in non-metals, *in* Johnson, R. A., and Orlov, A., eds., Physics of Radiation Effects in Crystals: Amsterdam, Elsevier, p. 387–469.

Dallmeyer, R. D., 1975, Incremental $^{39}Ar/^{40}Ar$ ages of biotite and hornblende from retrograde basement gneisses of the southern Blue Ridge and their bearing on the age of Paleozoic metamorphism: Am. Jour. Sci., v. 276, p. 444–460.

Davis, R. G., 1974, Pre-Grenville ages of basement rocks in central Virginia: a model for the interpretation of zircon ages: Unpub. M.S. thesis, Virginia Polytechnic Institute and State University, Blacksburg, 47 p.

Dirks, P., and Hand, M., 1991, Structural and metamorphic controls on the distribution of zircon in an evolving quartzofeldspathic migmatite: an example from the Reynolds Range, central Australia: Jour. Metamor. Geol., v. 9, p. 191–202.

Duchesne, J. C.; Caruba, R.; and Iacconi, P., 1987, Zircon in charnockitic rocks from Rogaland (southwest Norway): petrogenetic implications: Lithos, v. 20, p. 357–368.

Gehrels, G. E., and Saleeby, J. B., 1987, Geology of southern Prince of Wales Island, southeastern Alaska: Geol. Soc. America Bull., v. 98, p. 123–137.

Gebauer, D., and Grunenfelder, M., 1976, U-Pb zircon and Rb-Sr whole rock dating of low-grade metasediments, example: Montagne Noire (Southern France): Contrib. Mineral. Petrol., v. 39, p. 13–32.

Hansen, B. T., and Friderichsen, J. D., 1989, The influence of recent lead loss on the interpretation of disturbed U-Pb systems in zircons from igneous rocks in east Greenland: Lithos, v. 23, p. 209–223.

Holland, H. D., and Gottfried, D., 1955, The effect of nuclear radiation on the structure of zircon: Acta Cryst., v. 8, p. 291–300.

Krogh, T. E., 1973, A low contamination method for hydrothermal decomposition of zircon and extraction of U and Pb for isotopic age determinations: Geochim. Cosmochim. Acta, v. 37, p. 485–494.

Lancelot, J. R.; Boullier, A. M.; Maluski, H.; and Ducrot, J., 1983, Deformation and related radiochronology in a late Pan-African mylonite shear zone, Adrar des Iforas, Mali: Contrib. Mineral. Petrol., v. 82, p. 312–326.

Lindh, A., and Schoberg H., 1988, A tentative study of the U-Pb isotope system in zircon from the Mylonite Zone, southeast Norway: Geol. Foren. Stockholm Forh., v. 110, p. 15–20.

Lloyd, G. E., 1987, Atomic number and crystallographic contrast images with the SEM: a review of backscattered electron techniques: Mineral Mag., v. 51, p. 3–19.

———, and Ferguson, C. C., 1981, Boudinage structure: some new interpretations based on elastic-plastic finite element simulations: Jour. Struct. Geol., v. 3, p. 117–128.

Ludwig, K. R., 1990*a*, ISOPLOT for MS-DOS: a plotting

and regression program for radiogenic isotope data, for IBM-PC compatible computers, Version 2.11: U.S. Geol. Survey Open File Rept. 88-557, 33 p.

———, 1990*b*, PBDAT for MS-DOS: a computer program for IBM-PC compatibles for processing raw Pb-U-Th isotope data, Version 1.07: U.S. Geol. Survey Open File Rept. 88-542, 34 p.

Mitra, G., 1978, Ductile deformation zones and mylonites: the mechanical processes involved in the deformation of crystalline basement rocks: Am. Jour. Sci., v. 278, p. 1057–1084.

Murakami, T.; Chakoumakos, B. C.; Ewing, R. C.; Lumpkin, G. R.; and Weber, W. J., 1991, Alpha-decay event damage in zircon: Am. Mineral., v. 76, p. 1510–1532.

Ozkan, H., 1976, Effect of nuclear radiation on the elastic moduli of zircon: Jour. Appl. Phys., v. 47, p. 4772–4779.

Paterson, B. A.; Stephens, W. E.; and Herd, D. A., 1989, Zoning in granitoid accessory minerals as revealed by backscattered electron imagery: Mineral. Mag.,v. 53, p. 55–61.

Peterman, Z. E.; Zartman, R. E.; and Sims, P. K., 1986, A protracted Archean history in the Watersmeet Gneiss Dome, northern Michigan, *in* Shorter Contributions to Isotope Research: U.S. Geol. Survey Bull. 1622, p. 51–64.

Pettingill, H. S.; Sinha, A. K.; and Tatsumoto, M., 1984, Age and origin of anorthosites, charnockites, and granulites in the central Virginia Blue Ridge: Nd and Sr isotopic evidence: Contrib. Mineral. Petrol., v. 85, p. 279–291.

Pidgeon, R. T.; O'Neil, R. J.; and Silver, L. T., 1966, Uranium and lead isotopic stability in a metamict zircon under experimental hydrothermal conditions: Science, v. 154, p. 1538–1540.

Sahama, T. G., 1981, Growth structure in Ceylon zircon: Bull. Mineral., v. 104, p. 89–94.

Scharer, U., 1978, Rock deformation and zircon-sphene U-Pb dating, *in* Short Papers of the Fourth International Conference, Geochronology, Cosmochronology, Isotope Geology 1978: U.S. Geol. Survey Open File Rept. 78-701, p. 380–382.

Sinha, A. K., and Bartholomew, M., 1984, Evolution of the Grenville terrane in the central Virginia Appalachians: Geol. Soc. America Spec. Paper 194, p. 175–186.

———, and Glover, L., 1978, U-Pb systematics of zircons during dynamic metamorphism: Contrib. Mineral. Petrol., v. 66, p. 305–310.

———; Hewitt, D. A.; and Wayne, D. M., 1989, Hydrothermal stability of zircon: hydrothermal and isotopic studies, *in* Zircons and fluids: an experimental investigation with applications for radioactive waste disposal; Progress Rept. U.S. Department of Energy, Contract No. DE-FGOS-88 ER 13951-1 (Virginia Polytechnic Institute and State University, Dept. of Geological Sciences) p. 2–9.

Stacy, J. S., and Kramers, J. D., 1975, Approximation of terrestrial lead isotope evolution by a two-stage model: Earth Planet. Sci. Lett., v. 26, p. 207–221.

Steiger, R. H., and Jaeger, E., 1977, Subcommission on geochronology: convention on the use of decay constants in geo- and cosmo-chronology: Earth Planet. Sci. Lett., v. 36, p. 359–362.

Wayne, D. M., 1990, Isotopic systematics and mass transfer in amphibolite-grade mylonites: Unpub. Ph.D. dissertation, Virginia Polytechnic Institute and State University, Blacksburg, 324 p.

———, and Sinha, A. K., 1988, Physical and chemical response of zircons to deformation: Contrib. Mineral. Petrol., v. 98, p. 109–121.

———; ———; and Hewitt, D. A., 1992, Differential response of the zircon U-Pb system across a lithologic boundary: an example from the Hope Valley Shear Zone, southeastern Massachusetts, USA: Contrib. Mineral. Petrol., v. 109, p. 408–420.

White, S. H.; Burrows, S. E.; Carreras, J.; Shaw, N. D.; and Humphreys, F. J., 1980, On mylonites in ductile shear zones: Jour. Struct. Geol., v. 2, p. 175–187.